



Article

Application of the Electrochemical Permeation Method for Hydrogen Diffusion Coefficient Determination in Pipeline Steel 10G2

Vladislav I. Borodin ¹, Aleksandr V. Lun-Fu ¹, Victor N. Kudiiarov ², Andrey M. Lider ², Ivan S. Sakvin ² , Mikhail A. Bubenchikov ¹, Dmitry S. Kaparulin ³ and Vyacheslav A. Ovchinnikov ^{4,*} 

¹ LLC “Gazprom Transgaz Tomsk”, 9 Frunze Street, 634029 Tomsk, Russia; vi_borodin@mail.ru (V.I.B.); lunfu_av@mail.ru (A.V.L.-F.); michael121@mail.ru (M.A.B.)

² Division for Experimental Physics, National Research Tomsk Polytechnic University, 634050 Tomsk, Russia; kudiyarov@tpu.ru (V.N.K.); lider@tpu.ru (A.M.L.); sakvinis@gmail.com (I.S.S.)

³ Department of Quantum Field Theory, National Research Tomsk State University, 36 Lenin Ave., 634050 Tomsk, Russia; dsc@phys.tsu.ru

⁴ Department of Physical and Computational Mechanics, National Research Tomsk State University, 36 Lenin Ave., 634050 Tomsk, Russia

* Correspondence: empiric@mail.ru

Abstract: In this article, we conduct research on the effect of corrosion tests on the hydrogen diffusion process in gas steel in electrochemical permeability tests. This tests show that a long corrosion test time reduces the hydrogen diffusion coefficient by an order of magnitude, indicating the formation of aging defects in the steel. During operation, the diffusion coefficient decreases by two orders of magnitude, which also indicates the formation of a large number of defects in the steel. Consequently, based on the change in the diffusion coefficient in the material, it is possible to assess the degree of material failure.

Keywords: pipeline steel; corrosion testing; electrochemical permeation method; hydrogen diffusion; diffusion coefficient



Citation: Borodin, V.I.; Lun-Fu, A.V.; Kudiiarov, V.N.; Lider, A.M.; Sakvin, I.S.; Bubenchikov, M.A.; Kaparulin, D.S.; Ovchinnikov, V.A. Application of the Electrochemical Permeation Method for Hydrogen Diffusion Coefficient Determination in Pipeline Steel 10G2. *Coatings* **2021**, *11*, 1260. <https://doi.org/10.3390/coatings11101260>

Academic Editor: Ricardo Branco

Received: 31 August 2021

Accepted: 13 October 2021

Published: 16 October 2021

Publisher's Note: MDPI stays neutral with regard to jurisdictional claims in published maps and institutional affiliations.



Copyright: © 2021 by the authors. Licensee MDPI, Basel, Switzerland. This article is an open access article distributed under the terms and conditions of the Creative Commons Attribution (CC BY) license (<https://creativecommons.org/licenses/by/4.0/>).

1. Introduction

One of the most important scientific and technical problems of recent years is the problem of extending the life of the safe operation of gas pipelines due to the increased risk of technogenic accidents caused by insufficient operational reliability of the metal [1–3]. The most common type of damage to structural materials (such as steel, copper, aluminum, etc.) is corrosion [4]. The main cause of accidental destruction on trunk pipelines is stress corrosion cracking. The stress corrosion cracking caused accidents in at least 60% of cases in the period from 1991 to 2005 according to the data provided by Gazprom [5]. Any accident can lead to disastrous consequences for both the environment and human life. For example, 100 square meters of soil were contaminated during an accident at an oil pipeline in the Republic of Komi (Russia) in 1994. In this case, the costs of eliminating the consequences amounted to more than 100 million US dollars [6,7]. Another example is the accident of a gas pipeline in Louisiana (USA) where 17 people died [8]. The cause of these accidents is the stress corrosion cracking, caused by the aging of the pipeline metal. In this regard, the study of the stress corrosion cracking in pipeline steels is of great interest.

The widespread use of steel 10G2 as a single-seam welded pipe for the main pipeline is due to its characteristics such as high strength and ductility; high corrosion and mechanical strength; high reliability with static, cyclic and dynamic effects; resistance to ductile and brittle fracture at low temperatures down to −70 °C; the service life of materials is at least 25 years. Pipelines made of this steel are mainly used to transport oil, gas and other hydrocarbons. The composition of these elements contains hydrogen which,

penetrating deep into the material, leads to a distortion of the crystal lattice, which leads to hydrogen embrittlement of the first kind [9–11]. In addition, hydrogen is contained in the atmosphere, groundwater and salts, acids and alkalis dissolved in them. In pipeline steels, a high concentration of carbon is formed in the ferritic matrix to ensure high strength of the products. Such a structure dissolves in crystal defects over time due to the non-equilibrium state. In a corrosive environment, a microscopic galvanic couple arises near each micromixture, in which an impurity is the cathode, and the base metal is the anode, which is destroyed. Cementite is such an impurity in steel. All carbon can dissolve only on dislocations at low supersaturation. If the supersaturation is significant, and the number of dislocations is not enough to capture all carbon atoms, it also diffuses to the grain boundaries and accumulates there. Formation of secondary phases on grain boundaries can cause local microstresses, which lead to the formation of cracks. An increase in the number of cracks leads to a gradual destruction of the material. One approach to qualitatively assess the degree of damage to the material is the study of the permeability of hydrogen through the material.

Studies of the effect of various defects on hydrogen diffusion in steels have found wide application in the world. For example, Rivera et al. [12] in 2012 showed the dependence of hydrogen diffusion coefficient on the degree of cold rolling in pipe steel API 5L X60. It was shown that weak (reversible) hydrogen traps predominate in the steels. Hack et al. [13] in their study of the effect of the microstructure and composition of X70 steel on hydrogen permeability by the hydrogen electrochemical permeability method showed that the change in the number of alloying elements directly affects the diffusion of hydrogen. The authors suggest that the difference in diffusion coefficients is related to the difference in microstructure from the surface to the volume, as well as to the different number of dislocations. Drexler et al. [14], studying the fatigue failure of steels in air and in hydrogen environment, showed that API-X70 steel fails faster in hydrogen than in air. The authors attribute this to the penetration of hydrogen deep into the sample and subsequent accumulation in defects. Hydrogen accumulation in defects leads to an increase in interfacial microstresses and the appearance of microcracks. Olden et al. [15] investigated API-X70 pipeline steel for hydrogen diffusion and mechanical properties. The initial material, weld and heat-affected zone were investigated. The authors noted that the concentration of hydrogen in the studied samples did not exceed 1 ppm, which indicates a small accumulation of hydrogen in the steels. The fact that the weld has the lowest diffusion coefficient indicates that the martensitic structure is a delay factor. Hung M. Ha, Jia-He Ai and John R. Scully [16] in a study of the effect of cold work on diffusion and hydrogen trapping in API-X70 steel by electrochemical permeation determined that during deformation, mainly two types of hydrogen traps with activation energies of 8.9 and 14.9 kJ/mol are formed in the material. Traps with lower energies are reversible and correspond to dislocation lines or vacancies. Traps with higher activation energies can be dislocation piles, vacancies or a network of sessile dislocations, which are considered irreversible at room temperature.

These studies are extremely interesting and important for studying hydrogen diffusion in pipeline steels because they show the effect of defects formed during deformation on hydrogen diffusion. In the present work, a study of operating conditions on hydrogen diffusion was carried out. Three series of specimens were used for this purpose: the original steel, steel after accelerated corrosion testing and steel taken out of service as a result of an accident. Thus, the effect of defects formed during material aging and corrosion during operation was investigated.

Many kinds of defects in the crystal structure and various kinds of inclusions of secondary phases form in pipeline steels during operation, one of the criteria for assessing the degree of development of critical defective material structure can be considered the hydrogen diffusion coefficient in the material. This is since various types of defects are hydrogen capture centers and directly interfere with the diffusion of atoms in the material.

Therefore, since the hydrogen diffusion coefficient has an inverse time dependence, the smaller its value, the more defects there are in the material.

Currently, the problem of corrosion of gas pipelines is very well studied. Hydrogen embrittlement is distinguished, among other things, as a corrosion mechanism leading to a special type of corrosion, the so-called stress corrosion cracking. These mechanisms have been studied quite deeply, but the mechanism of the infinitely slow dissociation of the components of natural gas (methane) flowing through gas pipelines on their inner metal surface has never been considered before. An analogue of this process has long been well known in production—it is steam reforming of methane, where methane is dissociated to carbon and hydrogen in the presence of water vapor under the action of Fe, Ni, Co catalysts. The equations of chemical kinetics for these processes require a high temperature—about 600 K, however, they leave the possibility of such reactions occurring at 270 K, albeit at a very low rate. In this work, for the first time, it is the intrinsic dissociation of methane inside pipelines as a source of hydrogenation of the metal of their inner surface that is investigated. Estimates show that the positive hydrogen ions released as a result of methane dissociation are readily captured by the metal surface, which has a lower electrochemical potential, and over the years of operation, they allow accumulating a significant amount of hydrogen, which undoubtedly leads to hydrogen embrittlement of pipeline steel as such and to the manifestation of this embrittlement in the form stress corrosion cracking.

There are several methods for studying hydrogen diffusion through metal membranes. One of such methods is the study of diffusion by electrochemical penetration. The use of this method is implemented in many experimental installations [17–19]. The advantage of this method is its simplicity and the possibility of studying hydrogen diffusion in aggressive media. The disadvantages are that in this method it is not possible to change the temperature of the experiment.

Another similar method of studying hydrogen diffusion through metal membranes can also be distinguished. The main difference from the previous method is the use of a mass spectrometer as an identifier of released hydrogen. The operating principle of the experimental setup for studying hydrogen permeability through a metal membrane by electrochemical permeation and mass spectrometric analysis [20,21] is as follows. The metal foil under study is placed between two compartments, which are hermetically secured due to the design of the setup. When the circuit is closed, direct current flows through the electrolyte in the first compartment, as a result of which hydrogen ions are released again on the metal membrane, which is the cathode, and the acidic residue is deposited on the anode. Over a period, due to diffusion processes, hydrogen penetrates deep into the crystalline structure of the membrane and passes through its entire thickness, thereby entering the second compartment of the high-vacuum chamber. An important feature of this method is the possibility of studying the interaction of hydrogen isotopes and metals.

Another method of studying the permeability of hydrogen through metal membranes has also been implemented in many experimental facilities [22,23]. An important distinguishing feature of which is the study of the interaction of metals with hydrogen in the gas phase. Experimental complexes of this type can be used to study the effect of various one-way hydrogenation processes of a metal membrane on various protective coatings using a wide range of different saturation parameters, which contributes to an even deeper study of metal-hydrogen systems. In contrast to previous installations, the implementation of this type of unit is more expensive.

In this article the possibility of using the diffusion coefficient as a criterion for the degree of pipeline material degradation during operation is tested. As studies have shown, accelerated corrosion tests lead to a change in the diffusion coefficient by 1 order of magnitude, which is associated with the formation of oxides and accumulation of hydrogen. During 25 years of pipeline operation, redistribution of carbon and formation of secondary cementite phase occur in the material, which leads to changes in the diffusion coefficient by 2 orders of magnitude.

2. Materials and Methods

In this work, we used the electrochemical method for studying the diffusion of hydrogen. The method consists in the following: a metal test membrane is placed between two electrochemical compartments, which is hermetically fixed. When direct current flows through the electrolyte, in the anode compartment, hydrogen ions are released on the surface of the test sample acting as the cathode and the acid residue is deposited on the anode. Hydrogen ions deposited on the surface diffuse into the bulk of the material and, after a certain period, are separated from the reverse side into another compartment, where they are deposited on the reference electrode. In this method, to find the hydrogen permeability parameters, it reduces to solving the Fick Equations (1) and (2) [24] with boundary conditions of the first kind (3):

$$J = -D \frac{\partial C}{\partial x}, \text{ m}^2/\text{s} \quad (1)$$

$$\frac{\partial C}{\partial t} = D \frac{\partial^2 C}{\partial x^2}, \quad (2)$$

$$\begin{cases} C|_{t=0} = 0, 0 \leq X \leq l, \\ C|_{t \geq 0} = S_H \sqrt{P_0}, X = 0, \\ C|_{t \geq 0} = 0, X = l. \end{cases} \quad (3)$$

when C is concentration, J is flow, S_H is hydrogen solubility, P_0 is hydrogen pressure, l is thickness of membrane.

At the input side of the sample, a concentration equal to the equilibrium solubility is instantly established, and at the initial side of the sample, the hydrogen concentration is zero.

In accordance with Fick's first law, the flow of hydrogen through a unit area membrane is written as follows:

$$J = \frac{DS_H}{l} \left\{ 1 + 2 \sum_{n=1}^{\infty} \left[\cos\left(\frac{\pi n}{l} x\right) \exp\left(-\frac{D\pi^2 n^2}{l^2} t\right) \right] \right\}. \quad (4)$$

For the flow on the output side of the membrane (J_{out}), based on the first Fick law, we have the expression:

$$J_{out} = \frac{DS_H}{l} \left\{ 1 + 2 \sum_{n=1}^{\infty} \left[(-1)^n \exp\left(-\frac{D\pi^2 n^2}{l^2} t\right) \right] \right\} \quad (5)$$

To calculate the diffusion coefficient, use a stationary flow value (J_{st}) having the following expression:

$$J_{st} = J(t, l)|_{t \rightarrow \infty} = \frac{DS_H}{l}. \quad (6)$$

Studying the dependence $J(t)$, we can distinguish the characteristic point, this is the time of establishment of half of the stationary flow $t_{0.5}$ (Figure 1).

To calculate the diffusion coefficient, it is necessary to use the following formula [25]:

$$D = \frac{l^2}{6t_{0.5}}, \quad (7)$$

where l is membrane thickness.

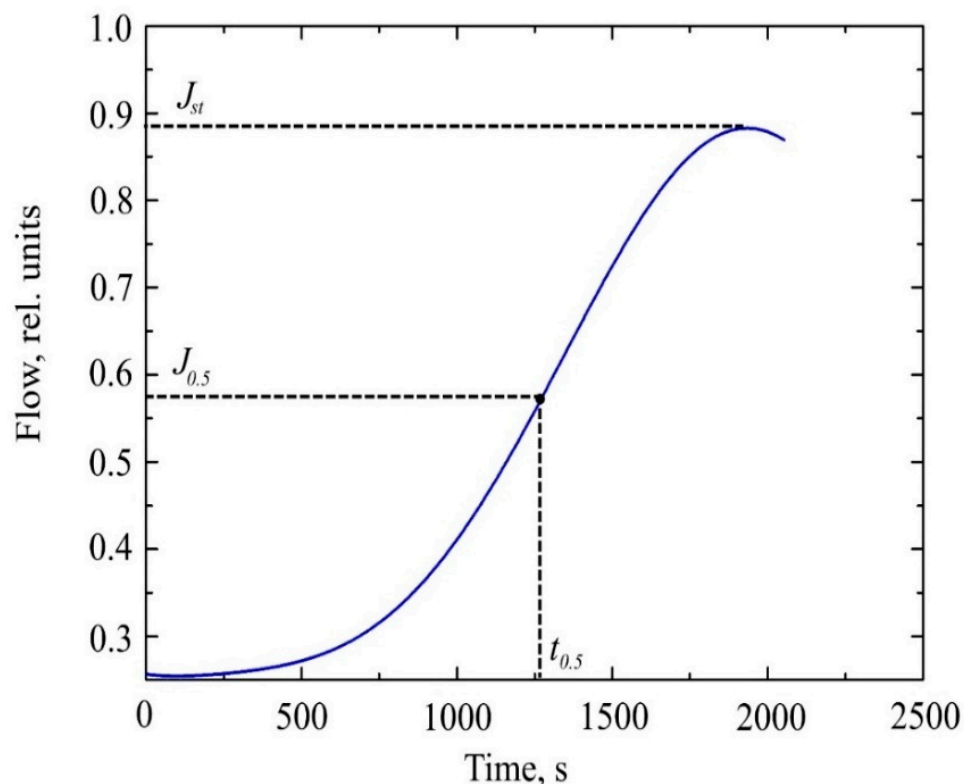


Figure 1. The curve of hydrogen permeability through a metal membrane.

The experimental installation Stand for Testing Electrochemical Permeation (STEP) for studying hydrogen permeability through metal membranes by electrochemical penetration is used to study hydrogen diffusion in metals, as well as to study the metal-hydrogen system as a whole [26]. In addition, using the experimental complex, it is possible to study the influence of various modes of unilateral hydrogenation of a metal membrane on various protective coatings, the kinetics of defect formation in the surface layer of a metal. The hydrogen permeability research facility allows one to confirm fundamental hypotheses, as a rule, created to explain experimental data.

The study of hydrogen permeability through metal membranes using the STEP experimental bench allows one to determine the diffusion coefficient of hydrogen in the material under study, i.e., the time of diffusion of hydrogen ions through a membrane of a certain thickness. In addition, using this stand, it is possible to study the effect of various protective coatings, various surface conditions and sample volume on the kinetics of hydrogen diffusion. By analyzing the experimental data and using an additional set of various experimental devices, it is possible to determine the degree of saturation of the material with hydrogen.

The chemical reaction processes taking place in this study at the STEP experimental bench in a 20% solution of sodium hydroxide NaOH are shown in Figure 2. The current density is selected to minimize the formation of gas bubbles on the sample surface. In this work, the current was approximately $\approx 300 \text{ mA/cm}^2$.

The passage of hydrogen ions through the material was determined by a change in the charge of the reference electrode in the near-surface region, as well as by a change in the chemical compositions of the near-surface region of the electrode during its interaction with hydrogen. The electrode potential of the surface of the sample and the reference electrode introduced into the cell was used as a measured, which makes it possible to judge the change in the charge state of the “output” region of the sample under study.

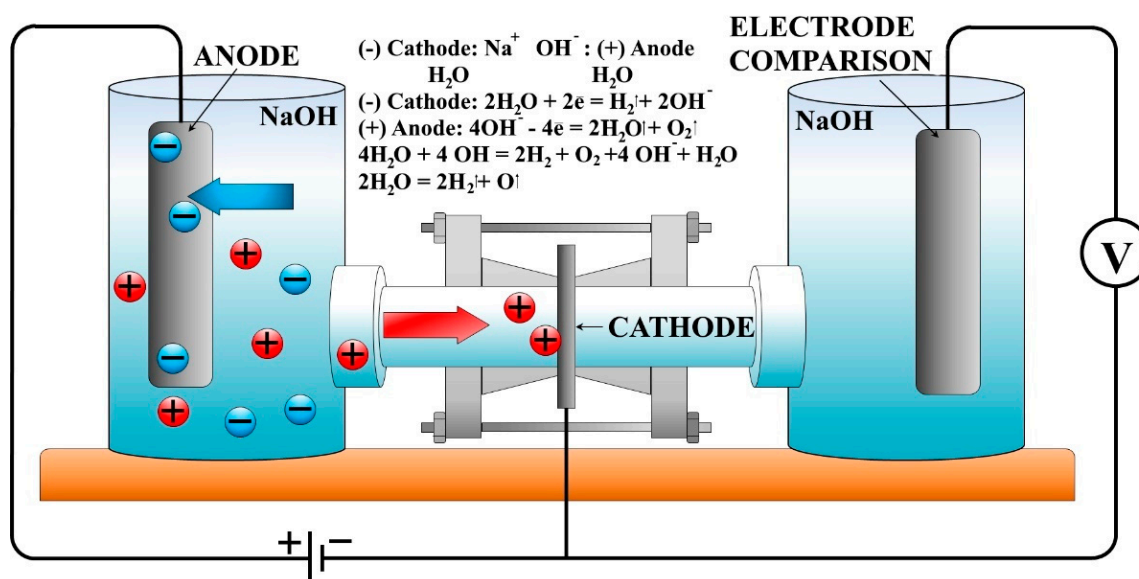


Figure 2. The processes of chemical reactions that occur during the electrochemical penetration of hydrogen ions through a metal membrane in a 20% solution of sodium hydroxide NaOH.

Steel grade 10G2 refers to stainless alloy steel, which is designed for the manufacture of highly loaded parts operating in torsion and bending under dynamic load, as well as in aggressive acidic environments with a high content of salts of alkali and alkaline earth metals, salts of nitric and sulfuric acids, chlorine ions, hydrogen sulfide. Steel has the following chemical composition (Table 1).

Table 1. Chemical composition of steel 10G2 (mass. %).

C	Si	Mn	Ni	S	P	Cr	Cu	Fe
0.07–0.15	0.17–0.37	1.2–1.6	0.03	0.035	0.035	0.3	0.3	97

Steel of this brand has found wide application in the manufacture of main pipelines since it has good mechanical properties (Table 2), a sufficiently high service life (at least 25 years) and has no restrictions on weldability.

Table 2. Mechanical properties of steel grade 10G2 at $T = 20^\circ\text{C}$.

$\sigma_{0.2}$, (MPa)	TS, [MPa]	δ , [%]	HB
265	470	21	197

Samples for studying the elemental and structural-phase composition, as well as for studying diffusion, were cut by spark cutting from the central part of the workpiece perpendicular to the axial direction of the pipe.

To study diffusion in 10G2 steel, a series of samples were prepared:

series #0—steel in its original state;

series #1—steel after testing in a gas atmosphere with moisture + heating;

series #2—steel after decommissioning of a part of the pipeline due to emergency conditions.

The steel sample in the initial state was cut out of the pipeline without the use of a reactor with methane supply. For sample #1, tests were carried out for 24 h under aggressive conditions of a gas environment with moisture and heating. A gas feed reactor (methane, “Gazprom Transgaz Tomsk”, Tomsk, Russia) was used to simulate the effect of an aggressive environment [27]. A predetermined amount of methane is fed into the tank. Gas passes through the sector of the studied pipe located in the tank, such as how

gas is supplied through the pipeline underground. From the outside the sector, oxygen, humidified air or another gas/liquid may be supplied. This device allows you to simulate the external impact of raw soil on the casing of the pipeline. The sample heating system allows accelerated corrosion tests at various temperatures. Sample #2 has been in operation for 25 years.

To study the structural phase and elemental composition, all samples were subjected to preliminary rough surface cleaning to remove the oxide film using sandpaper ISO 1000. In hydrogen diffusion experiments, sandpaper had to be thinned to a thickness of $300 \pm 30 \mu\text{m}$ using abrasives with a grit size of ISO 240, 800, 1500, 2500 in order. The final processing of the material was etching in a solution of hydrofluoric acid (HF) for 40 s.

3. Results and Discussion

The microstructure was studied by ion etching of the surface in argon. As can be seen from Figure 3, the grain is crushed during aging. This is since during operation the pipeline material experiences variable loads due to fluctuations in the pressure of the pumped gas. Therefore, in the samples of series #0, the average grain size is $d = 8.9 \mu\text{m}$; and in the samples subjected to corrosion tests—4.8 and 4.1 microns for series #1 and series #2, respectively. Furthermore, in the process of aging, the formation of carbide-like inclusions of the secondary phase occurs. Since the formation of carbide-like secondary phases is limited to a greater extent by the diffusion process of mass transfer of carbon atoms, it can be noted that the number of such inclusions is directly related to the operating time.

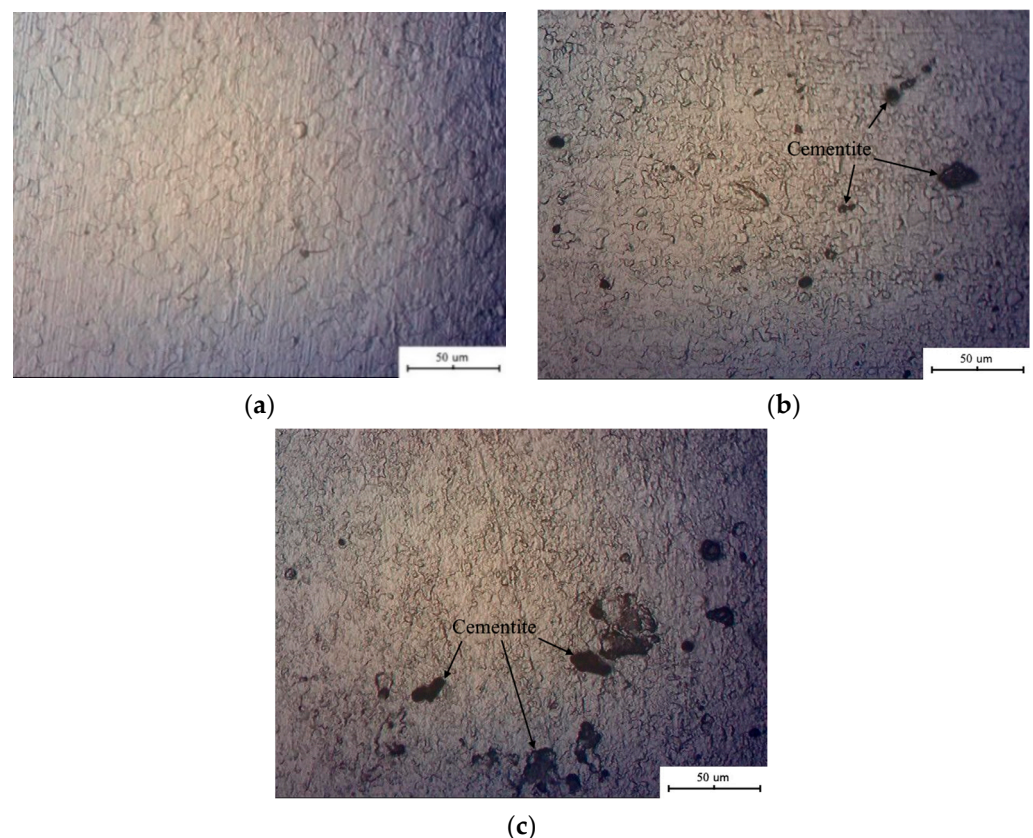


Figure 3. Microstructure of the surface of steel grade 10G2: (a) steel in its original state; (b) steel after accelerated corrosion testing; (c) steel decommissioned.

An initial sample of structural alloy steel 10G2, cut from a gas pipe before and after operation, as well as samples subjected to accelerated corrosion tests, were examined by scanning electron microscopy (SEM, Hitachi High-Tech Corporation, Kawasaki City, Japan) on a Hitachi S-3400N microscope with an energy dispersive spectrometer. This

microscope is equipped with an SE (secondary electrons) detector and a back scattered electrons (BSE) detector.

Figure 4 shows the studied initial sample of 10G2 steel (#1). This sample was cut from a natural gas pipeline. To analyze the sample using a scanning electron microscope, a relatively flat, undamaged surface area was selected.

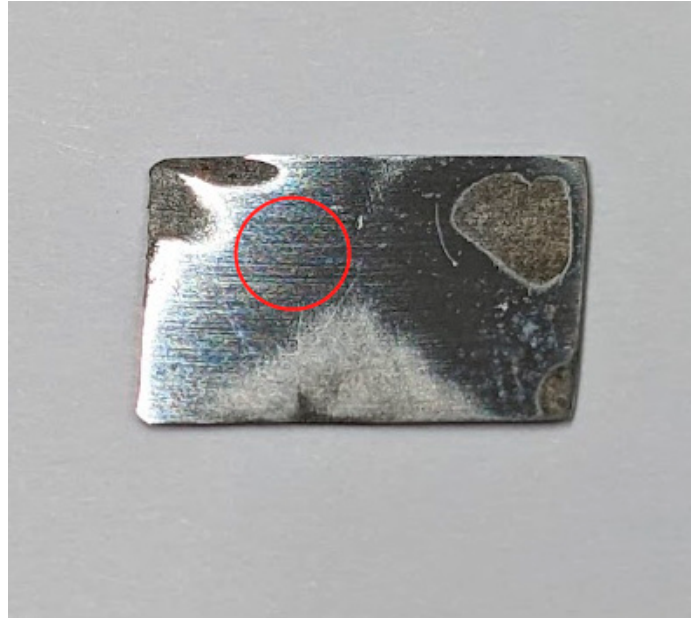


Figure 4. Photo of the surface of a 10G2 steel sample. The area in which the observations were made using a scanning electron microscope is shown in red.

A micrograph of the surface of the initial sample of steel 10G2 is shown in Figure 5.

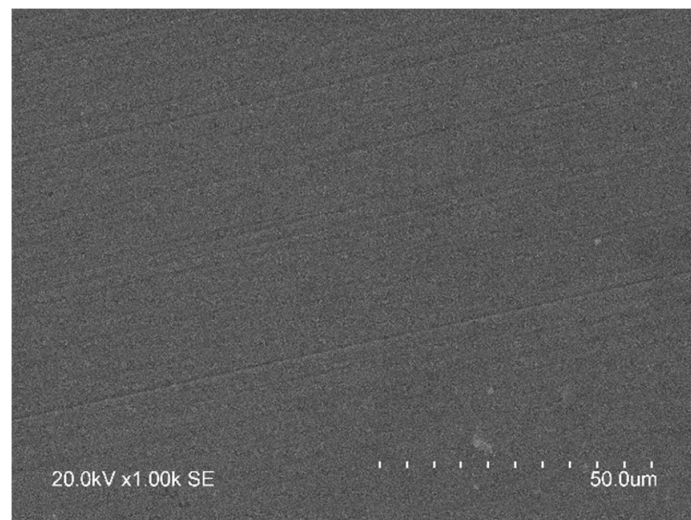


Figure 5. Micrograph of the surface of a sample of steel 10G2 (SE).

This micrograph shows that the sample surface is relatively flat. There are shallow, up to 2 μm in depth, traces left on the surface after the polishing procedure.

A micrograph of the surface of the initial steel sample obtained by registering backscattered electrons, as well as maps of elements are shown in Figure 6a–h.

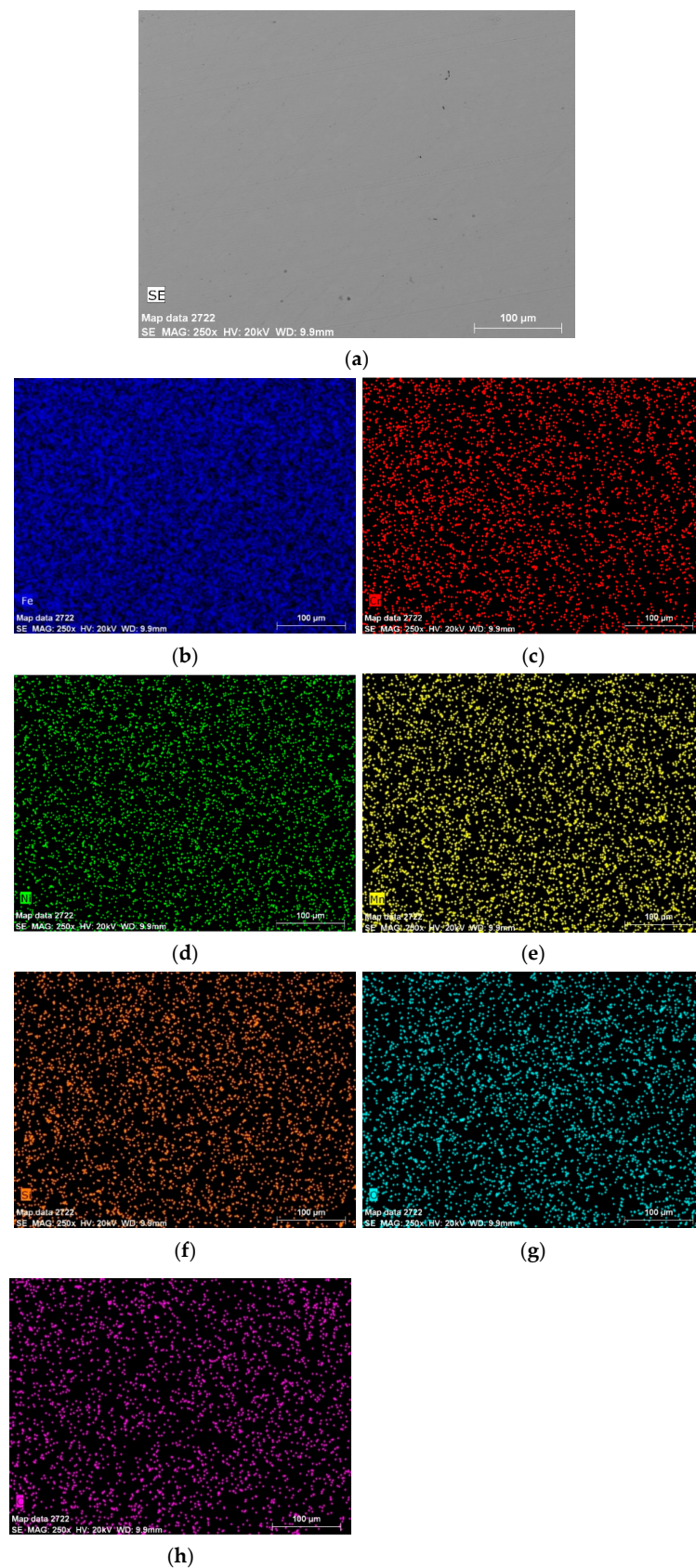


Figure 6. Micrograph of the surface of a sample of steel 10G2 (BSE) (a) and maps of the distribution of elements, (b) iron, (c) chromium, (d) nickel, (e) manganese, (f) silicon, (g) oxygen, (h) carbon.

Based on the micrograph of the sample surface, it can be concluded that the surface is homogeneous in composition. According to the maps of the distribution of elements, the sample corresponds to the chemical composition of steel grade 10G2 and consists of an alloy of iron, manganese, chromium and nickel. Oxygen (iron oxides and other substances) and carbon, which are surface contaminants, are present in small amounts. Silicon, which was found in small amounts over the entire surface during the study of this sample, was concentrated in some dark areas, which are a contaminant on the surface of the sample, as well as in a few voids. This contaminant may be nothing more than the residues of the cutting fluid used in the forming and testing of the pipeline.

Figure 7 shows a micrograph of the sample surface (Figure 7a) with spectra obtained by energy dispersive X-ray spectroscopy (EMF, Hitachi High-Tech Corporation, Kawasaki City, Japan) (Figure 7b,c).

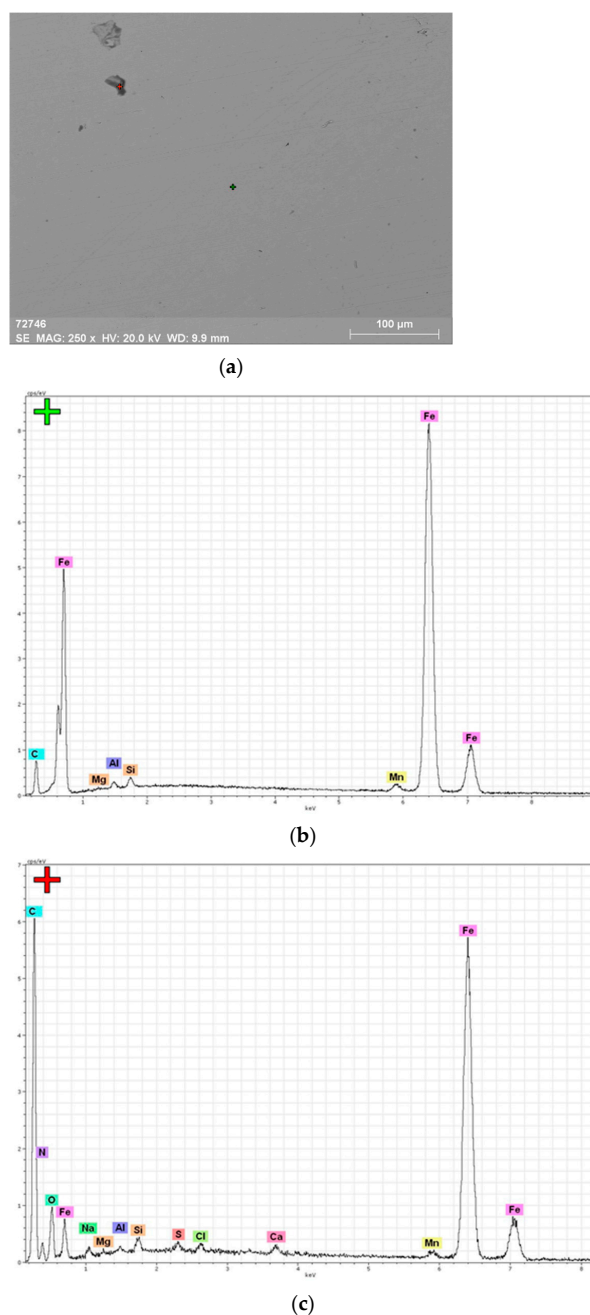


Figure 7. Micrograph (a) with EMF spectra (b,c) of the surface for a sample of steel 10G2.

The EMF results indicate that the sample surface does not contain any impurities, except for aluminum, which was recorded in an extremely small amount in the sample composition. The few dark areas on the surface that are associated with contaminants include carbon, oxygen, sodium, sulfur, chlorine, silicon and calcium.

Figure 8 shows a photograph of the surface of a 10G2 steel sample exposed to the corrosive effect of a gas environment and moisture (#2). The observation was carried out in an uncontaminated area bordering the visually corroded area.



Figure 8. Photo of a 10G2 steel sample exposed to an aggressive humid gas environment. The area of observation is shown in red.

Figure 9 shows a micrograph of the surface of a sample (Figure 9a) held in a corrosive environment of moisture and gas, as well as damage to the surface near the corrosion products (Figure 9b).

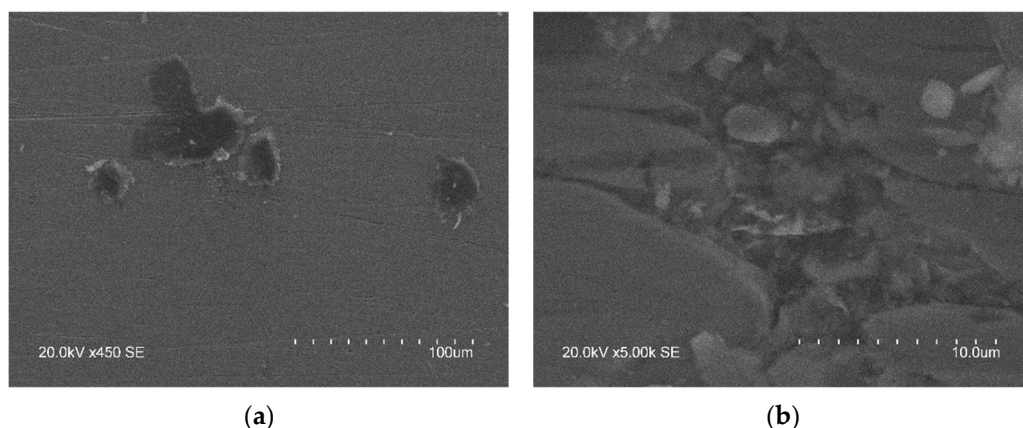


Figure 9. Micrograph of the surface of a sample of steel 10G2 (a), held in a humid atmosphere (SE) and the area of surface damage (b).

According to the above micrograph, there are traces on the surface after polishing. Corrosion precipitates and areas with damaged surfaces are observed, and such areas are observed over the entire surface of the sample.

A micrograph of the surface and maps of the distribution of elements for a steel sample, which was exposed to moisture and an aggressive gas environment, was obtained by registering backscattered electrons (Figure 10a–h).

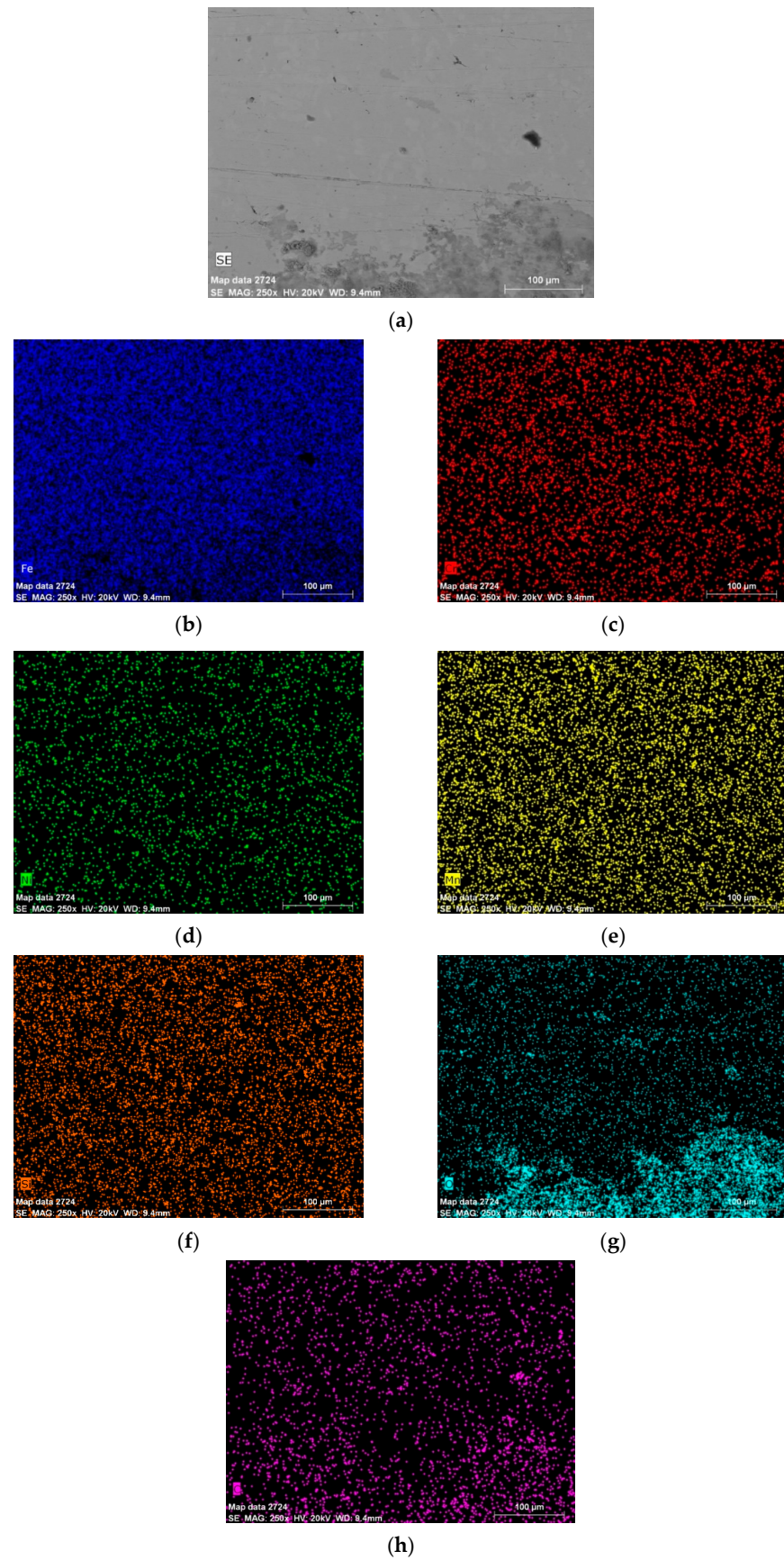
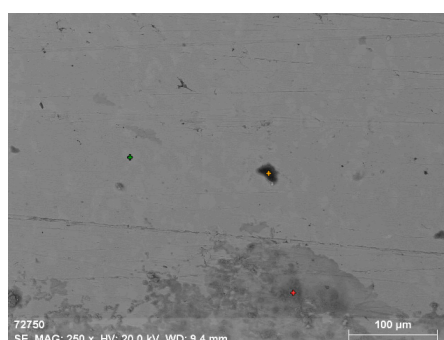


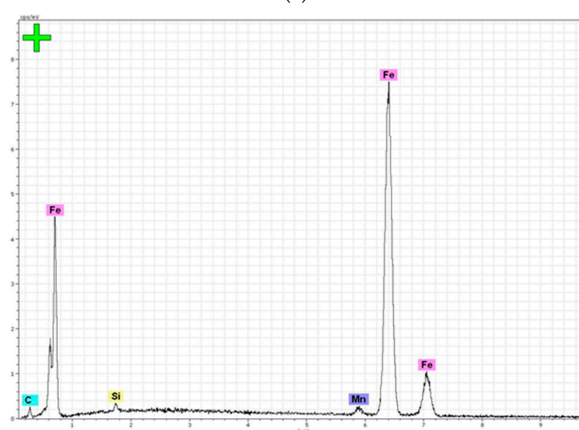
Figure 10. Micrograph of the surface of a 10G2 (BSE) steel sample (a) exposed to moisture and an aggressive gas environment, and a map of the distribution of elements, (b) iron, (c) chromium, (d) nickel, (e) manganese, (f) silicon, (g) oxygen, (h) carbon.

Based on the micrograph of the sample surface and the distribution maps of the elements, it can be concluded that the surface is heterogeneous in composition due to the numerous regions where Fe_2O_3 and Fe_2O_3 deposits (rust) are present. In these areas, there is an increased amount of oxygen and carbon, which is concentrated in the pores and voids that have arisen due to the aggressive effects of gas and moisture. In addition, even in areas without the release of corrosion products, numerous cracks, deep voids of small diameter and other damage are observed. The elements manganese, chromium and nickel are evenly distributed over the sample surface. Areas were observed in which a large amount of silicon is present.

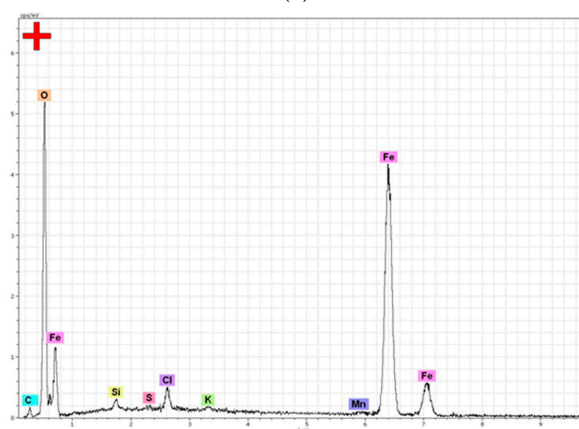
Figure 11 shows a micrograph of the sample surface (Figure 11a) with spectra obtained by energy dispersive X-ray spectroscopy (EDS) (Figure 11b–d).



(a)



(b)



(c)

Figure 11. Cont.

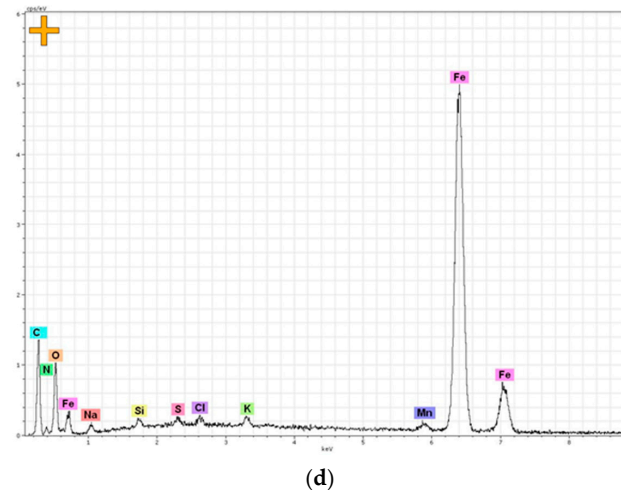


Figure 11. Micrograph (a) with EMF spectra (b–d) of the surface for a 10G2 steel sample exposed to moisture and an aggressive gas environment.

Based on the EMF results, it can be concluded that the sample surface does not contain any impurities. However, corrosion products are observed on the surface, consisting of iron oxides, as well as potassium and sodium. Contaminants are also present, including sodium, sulfur and potassium. Corrosion products consist of iron oxides and small amounts of potassium, silicon and sodium. It should be noted that chlorine, which is a well-known corrosion stimulant, has been found in corrosion products and in surface pollutants.

Figure 12 shows a photograph of the surface of a 10G2 steel sample cut from a previously operated gas pipeline (#3). The observation was carried out in a relatively unpolluted area.



Figure 12. Photo of a 10G2 steel sample cut from a previously operated gas pipeline. The area of observation is shown in red.

Figure 13 shows a micrograph of the surface of this sample at different magnifications.

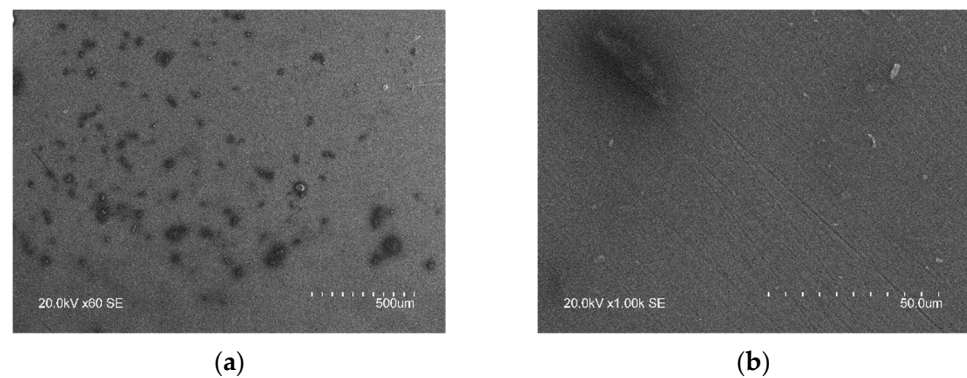


Figure 13. Micrograph of the surface of a 10G2 steel sample cut from a previously operated gas pipeline (SE) at 60 times (a) and 1000 times (b) magnification.

Based on these micrographs, the surface is heavily contaminated with foreign substances. There are traces of polish on the surface, as well as damage such as scratches, few pores and voids.

Figure 14 shows a micrograph of the surface (Figure 14a), obtained by registering backscattered electrons, as well as maps of the distribution of elements (Figure 14b–h).

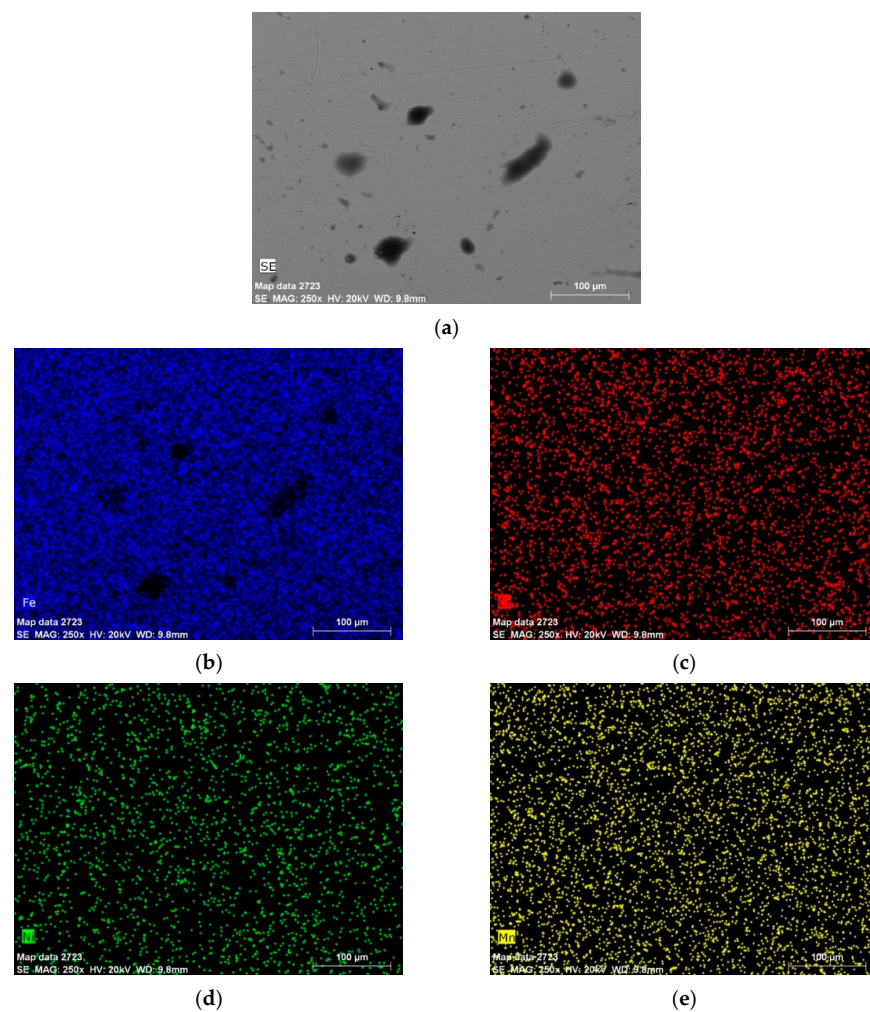


Figure 14. Cont.

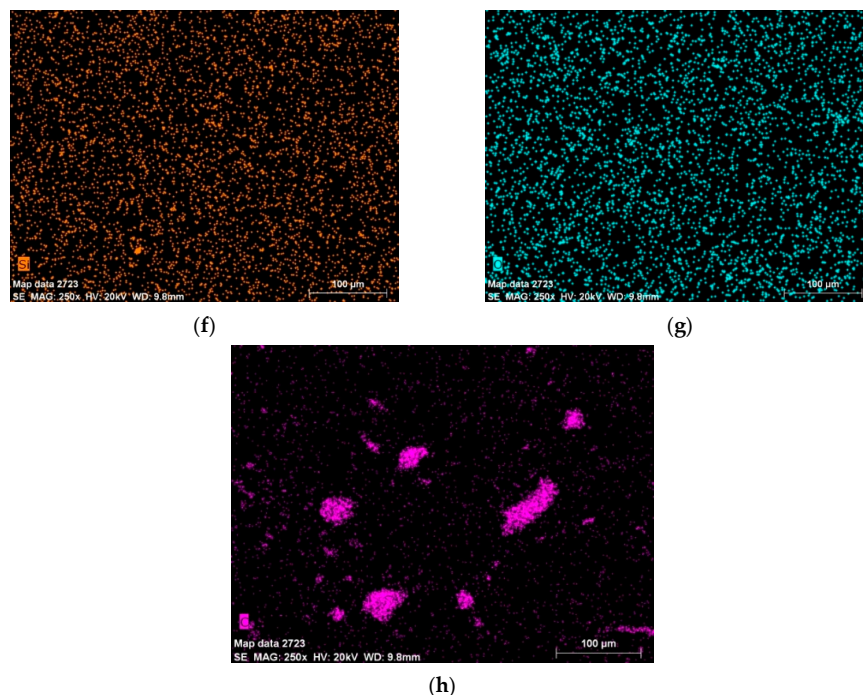


Figure 14. Micrograph of the surface of a 10G2 (BSE) steel sample (a) cut from a previously operated gas pipeline, and a map of the distribution of elements (b)iron, (c)chromium, (d)nickel, (e)manganese, (f)silicon, (g)oxygen, (h)carbon.

Based on the micrograph of the sample surface and the maps of the distribution of elements, it can be concluded that the surface is relatively homogeneous in composition, however, a large amount of polluting carbonaceous substances is present on the surface. The micrograph also shows small-diameter cavities. Alloying substances in steel are evenly distributed over the surface of the sample. Silicon has been found in small amounts in some areas with pollutants.

Figure 15 shows a micrograph of the sample surface (Figure 15a) with spectra obtained by energy dispersive X-ray spectroscopy (EDS) (Figure 15b,c).

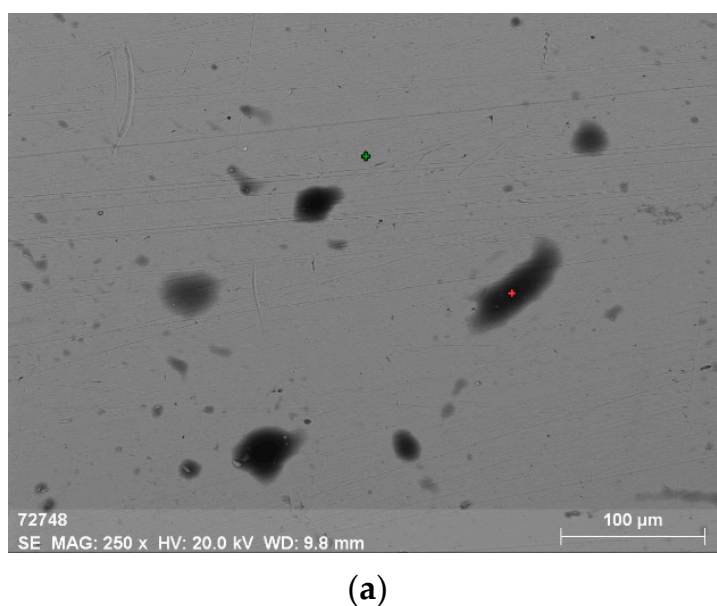
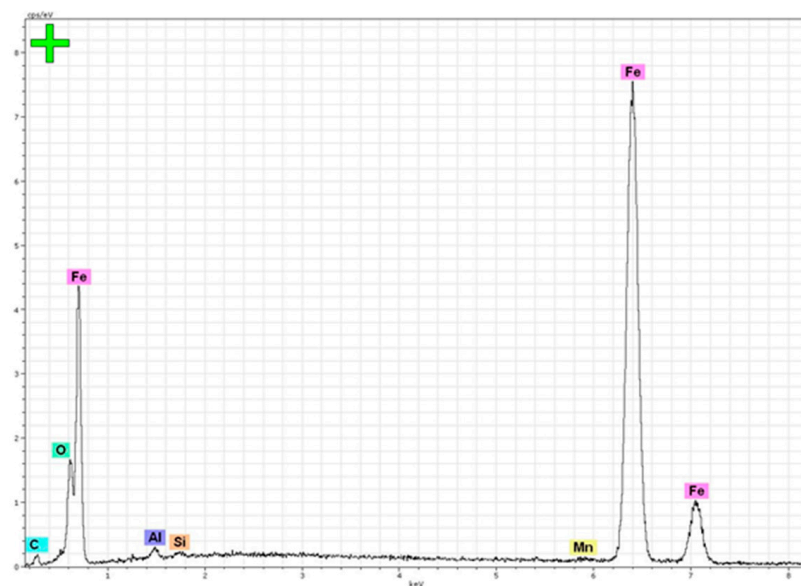
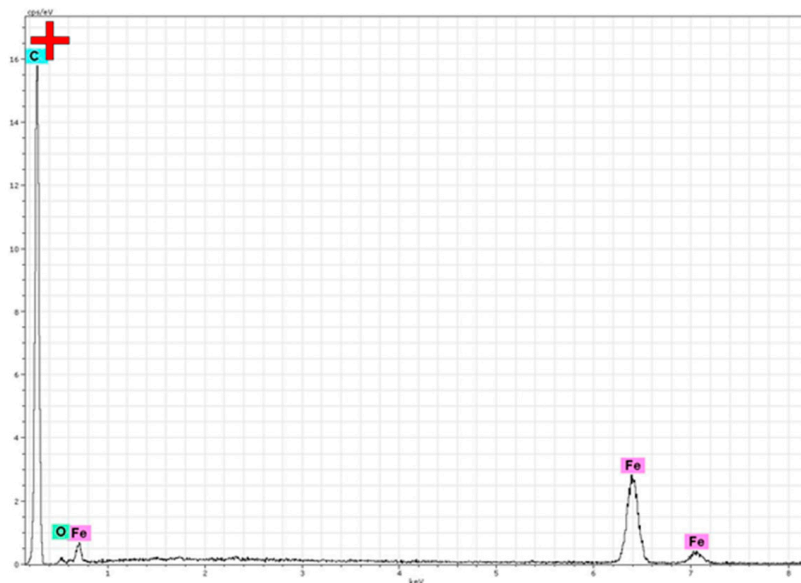


Figure 15. Cont.



(b)



(c)

Figure 15. Micrograph (a) with EDS spectra (b,c) of the surface for a 10G2 steel sample cut from a previously operated pipeline.

Based on the EDS results, it can be concluded that the sample surface does not contain any impurities, except for a certain amount of aluminum. In addition, a small amount of oxides is present on the surface. The contaminants are most likely carbon-based organic compounds.

The elemental composition of the steel was studied using a Glow Discharge Profiler 2 high-frequency glow discharge optical spectrometer. This laboratory complex combines a glow discharge excited by a radio frequency source and an optical emission spectrometer [28].

Studies of the elemental composition of steel grade 10G2 shows the following results (Table 3).

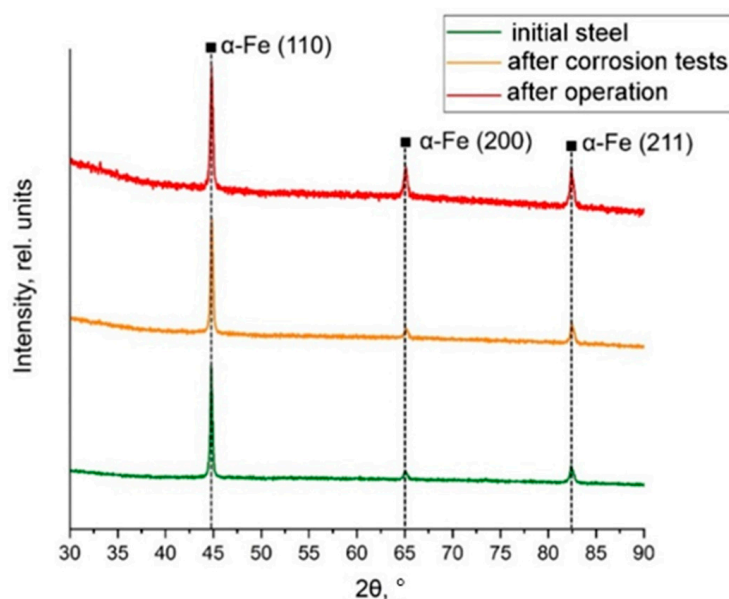
Table 3. The elemental composition of experimental samples of steel grade 10G2.

Element	Content, Mass. %		
	#0	#1	#2
C	0.056	0.060	0.051
Si	0.611	0.637	0.264
Mn	1.291	1.331	1.364
S	0.005	0.005	0
Cr	0.017	0.017	0.021
Fe	98.020	97.950	98.300

Elemental analysis shows that there is no significant difference between the test samples. Small deviations in the samples of series #2 in the content of silicon and sulfur can be associated with a change in the technology for the production and quality control of steel over a period of about 25 years.

The structural-phase composition of the steel was studied using a Shimadzu XRD 7000S diffractometer (Shimadzu Corporation, Kyoto, Japan) with the following parameters: range of angles is 10° – 90° , scan step is 0.0143, accumulation at a point of 2.149 s. Diffraction patterns were obtained using Cu $K\alpha_1/\alpha_2$ radiation.

Figure 16 shows the diffraction patterns for steel in its original state, steel after accelerated corrosion tests and steel decommissioning ambassadors.

**Figure 16.** Diffraction patterns of a series of experimental samples of steel grade 10G2.

Analysis of the diffraction pattern of all samples shows the presence of only the alpha-iron phase with a body-centered cubic crystalline modification. Cell parameters are presented in Table 4.

Table 4. The results of the structural-phase analysis of experimental samples of steel grade 10G2.

Parameters	#0	#1	#2
Detected phases	α -Fe_VCC	α -Fe_VCC	α -Fe_VCC
The content of phases, vol. %	100	100	100
Interplanar distance d , Å	2.0271	2.0254	2.0280
Lattice parameter a , Å	2.867	2.864	2.868

Based on the presented results, the impact on steel of an aggressive environment and high pressure does not affect the elemental and structural-phase composition of steel. This allows you to use the diffusion coefficient of hydrogen as a parameter that determines the possibility of safe use of the pipeline.

Uniaxial tensile tests were performed on a Com Ten DFM-5000 (Com-Ten Industries, Pinellas Park, FL, USA) testing machine at room temperature.

Based on the data presented above, accelerated corrosion tests lead to significant degradation of mechanical properties: the proportionality, elasticity and fluidity limits are reduced by 20%; the value of the tensile strength decreases by 7% and the value of the maximum relative elongation decreases by 18%. This may indicate embrittlement of pipeline steel due to exposure to a corrosive environment.

The experimental samples were subjected to an experiment on the permeability of hydrogen with the following parameters: current density in the anode compartment $\approx 300 \text{ mA/cm}^2$; experiment time is 22 h. The resulting permeability curves are shown in Figure 17.

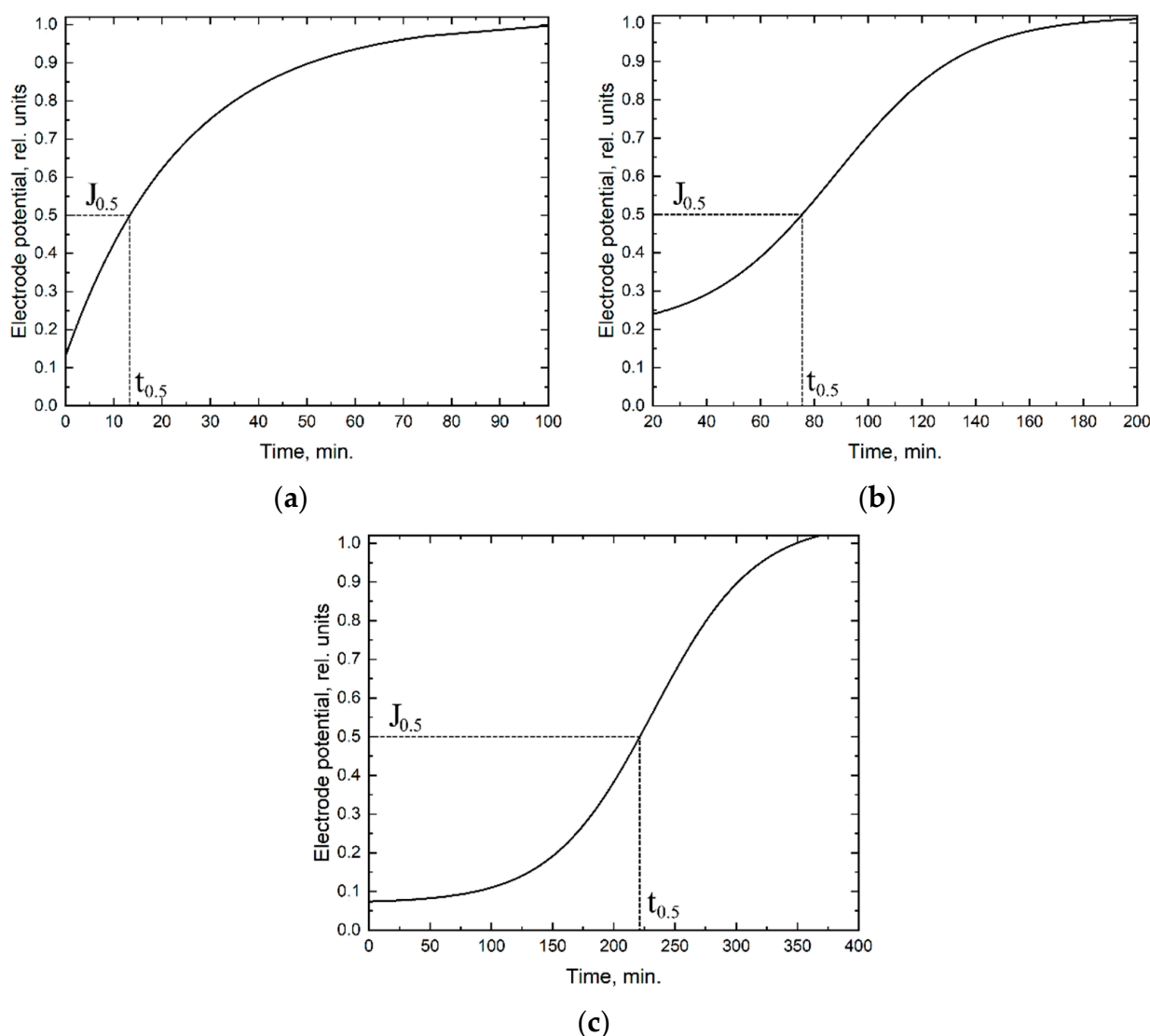


Figure 17. Hydrogen permeability curves: (a) steel in the initial state; (b) steel after accelerated corrosion testing; (c) steel decommissioned.

Using the previously described methodology for calculating the diffusion coefficient, the following data are obtained, presented in Table 5. The diffusion coefficient in the original steel lies in the range typical for this class of materials, which indicates the operability of

this methodology. The difference in diffusion coefficients in steels subjected to different operating parameters can be associated with the accumulation of many defects in the materials during operation. As is known, any defects in the crystal structure are hydrogen capture centers, which prevent the diffusion of hydrogen in the material.

Table 5. Diffusion parameters in experimental samples.

Parameter	Batch Number		
	#0	#1	#2
Sample Thickness, microns	330	330	280
The time to establish half of the stationary flow, min	13	78	225
Diffusion coefficient, cm ² /s	2.3×10^{-7}	3.9×10^{-8}	9.7×10^{-9}
Literature data of the diffusion coefficient [29–32], cm ² /s	2×10^{-7} – 5×10^{-6}	–	–

As noted in the papers above, the study of the effect of various defects on hydrogen diffusion is quite common. For example, in papers [12,16] the effect of cold rolling on hydrogen diffusion coefficient is investigated. At different degrees of rolling this value changes not more than 3 times. In [13] the effect of the number of alloying elements on the hydrogen diffusion coefficient is shown. In this work, the change in the diffusion coefficient is also observed not more than 3 times. The present paper investigates the effect of accelerated corrosion tests and real operating conditions on hydrogen diffusion in pipeline steel. Considering the results of microscopy and EDX in the material there is a redistribution of carbon and formation of secondary phases. Furthermore, the material accumulates oxygen with the formation of oxides and various gaseous impurities. The accelerated corrosion tests lead to a change in the diffusion coefficient by one order of magnitude, which indicates many different defects in the material. However, real operating conditions over long periods of time have a more significant effect on the diffusion coefficient. This is probably due to the diffusion rate of carbon in the iron, as indicated by the presence of more secondary cementite phases in the steel.

4. Conclusions

In this paper, a methodology has been developed to use the hydrogen diffusion coefficient as a criterion for assessing the degree of pipeline material degradation. Since any defects affect the mobility of hydrogen in the material, it is possible to qualitatively assess the damage obtained during operation.

To confirm material degradation during operation, metallographic, structural-phase and elemental analysis of 10G2 steel in different states was performed: initial material, material after accelerated corrosion tests and the material taken out of operation due to emergency condition. These studies show that the main mechanism of hydrogen diffusion rate change in the material is a reduction of grain size and release of second phase particles. Tensile tests show that defects accumulate in the material during aging, which leads to deterioration of mechanical characteristics.

Electron microscopy and EDX data show that oxides with weak carbide release form in the material subjected to accelerated corrosion tests. In the material that has been in service for 25 years, the carbide release is significantly higher. This may be due to the low diffusion rate of carbon in iron.

For the first time, it was shown that the study of hydrogen diffusion makes it possible to qualitatively estimate the degree of material degradation. In the original steel, the value of the diffusion coefficient is close to the literature data, which indicates the operability of this technique. In decommissioned steel due to an accident condition, the diffusion coefficient changes by two orders of magnitude, which confirms the formation of many aging defects. The change in the diffusion coefficient by one order of magnitude in the

steel subjected to accelerated corrosion tests indicates the possible appearance of aging defects during testing.

Author Contributions: Conceptualization, V.I.B. and A.V.L.-F.; methodology, V.N.K., M.A.B. and A.M.L.; experiment, I.S.S. and V.N.K.; analysis and investigation, V.N.K. and D.S.K.; writing—original draft preparation, A.M.L., V.N.K. and V.A.O.; writing—review and editing, V.N.K., M.A.B. and V.A.O. All authors have read and agreed to the published version of the manuscript.

Funding: This research was funded by the Program for Enhancing Competitiveness of National Research Tomsk Polytechnic University and by Governmental Program, Grant No. FSWW-2021-0017.

Institutional Review Board Statement: Not applicable.

Informed Consent Statement: Not applicable.

Data Availability Statement: Data is contained within the article.

Conflicts of Interest: The authors declare no conflict of interest.

References

1. Alamri, A.H. Localized corrosion and mitigation approach of steel materials used in oil and gas pipelines—An overview. *Eng. Fail. Anal.* **2020**, *116*, 104735. [CrossRef]
2. Shirband, Z.; Luo, J.-L.; Eadie, R.; Chen, W. Studying stress corrosion cracking crack initiation in pipeline steels in a near-neutral pH environment: The role of hydrotesting. *Corrosion* **2020**, *76*. [CrossRef]
3. Thodla, R.; Gui, F.; Holtam, C. Environmentally assisted cracking of subsea pipelines in oil & gas production environments—effect of static loading. *Corrosion* **2020**, *76*, 312–323. [CrossRef]
4. Ha, H.M.; Scully, J.R. Effects of phosphate on pit stabilization and propagation in copper in synthetic potable waters. *Corrosion* **2013**, *69*, 703–718. [CrossRef]
5. Medvedev, V.N.; Kuznetsov, V.V.; Shapiro, V.D.; Pochechuev, A.M.; Katz, I.D. On the causes of accidents in pipelines of main gas pipelines. In *Problems of Aging of Steel of Main Pipelines, Proceedings of the Scientific and Practical Seminar of LLC "FFPK MELAKS" and Physical and Technical Science Institute of UNN, Nizhny Novgorod, Russia, 23–25 January 2006*; Budzulyak, B.V., Sedykh, A.D., Eds.; University Book: Nizhny Novgorod, Russia, 2006; Available online: <https://elibrary.ru/item.asp?id=19646024> (accessed on 26 May 2020). (In Russian)
6. Kharionovsky, V.V.; Tcherni, V.P. Stress and Strain State of a Gas Pipeline in Conditions of Stress-Corrosion. In Volume 1: Regulations, Codes, and Standards; Current Issues; Materials; Corrosion and Integrity. In *Proceedings of the International Pipeline Conference*. American Society of Mechanical Engineers, Calgary, AB, Canada, 9–13 June 1996; pp. 479–483. [CrossRef]
7. Gaochao, L.; Steklov, O.I.; Shigo, S.; Papshev, E.I. A technique of the galvanic cathodic protection of welded joints in enameled pipelines. *Prot. Met. Phys. Chem. Surf.* **1999**, *35*, 221–224.
8. Shipilov, S.A.; Le May, I. Structural integrity of aging buried pipelines having cathodic protection. *Eng. Fail. Anal.* **2006**, *13*, 1159–1176. [CrossRef]
9. Gareev, A.G.; Nasibullina, O.A.; Rizvanov, R.G. Study of corrosion cracking of main gas and oil pipelines. *Oil Gas Bus.* **2012**, *6*, 126–146. (In Russian)
10. Neeraj, T.; Srinivasan, R. Hydrogen embrittlement of steels: Vacancy induced damage and nano-voiding mechanisms. *Corrosion* **2017**, *73*, 437–447. [CrossRef]
11. Kappes, M.; Frankel, G.S.; Thodla, R.; Mueller, M.; Sridhar, N.; Carranza, R.M. Hydrogen permeation and corrosion fatigue crack growth rates of X65 pipeline steel exposed to acid brines containing thiosulfate or hydrogen sulfide. *Corrosion* **2012**, *68*, 1015–1028. [CrossRef]
12. Castaño Rivera, P.; Ramunni, V.P.; Bruzzoni, P. Hydrogen trapping in an API 5L X60 Steel. *Corros. Sci.* **2012**, *54*, 106–118. [CrossRef]
13. Haq, A.J.; Muzaka, K.; Dunne, D.P.; Calka, A.; Pereloma, E.V. Effect of microstructure and composition on hydrogen permeation in X70 pipeline steels. *Int. J. Hydrog. Energy* **2013**, *38*, 2544–2556. [CrossRef]
14. Drexler, E.S.; Slifka, A.J.; Amaro, R.L.; Barbosa, N.; Lauria, D.S.; Hayden, L.E.; Stalheim, D.G. Fatigue crack growth rates of API X70 pipeline steel in a pressurized hydrogen gas environment: Fcgr of Api X70 pipeline steel in hydrogen gas. *Fatigue Fract. Eng. Mater. Struct.* **2014**, *37*, 517–525. [CrossRef]
15. Olden, V.; Alvaro, A.; Akselsen, O.M. Hydrogen diffusion and hydrogen influenced critical stress intensity in an API X70 pipeline steel welded joint—experiments and FE simulations. *Int. J. Hydrog. Energy* **2012**, *37*, 11474–11486. [CrossRef]
16. Ha, H.M.; Ai, J.-H.; Scully, J.R. Effects of prior cold work on hydrogen trapping and diffusion in API X-70 line pipe steel during electrochemical charging. *Corrosion* **2014**, *70*, 166–184. [CrossRef]
17. Zhao, W.; Zhang, T.; He, Z.; Sun, J.; Wang, Y. Determination of the critical plastic strain-induced stress of X80 steel through an electrochemical hydrogen permeation method. *Electrochim. Acta* **2016**, *214*, 336–344. [CrossRef]
18. El Alami, H.; Creus, J.; Feaugas, X. Influence of the plastic strain on the hydrogen evolution reaction on polycrystalline nickel electrodes in H₂SO₄. *Electrochim. Acta* **2006**, *51*, 4716–4727. [CrossRef]

19. Nikitenkov, N.N.; Khashkhash, A.M.; Shulepov, I.A.; Horuzhy, V.D.; Tyurin, Y.I.; Chernov, I.P.; Kudryavtseva, E.N. Installation for the study of radiation and thermal evolution of gases from inorganic materials. *Instrum. Equip. Exp.* **2009**, *6*, 110–115. (In Russian)
20. Nayeboossadri, S.; Speight, J.D.; Book, D. Hydrogen separation from blended natural gas and hydrogen by Pd-based membranes. *Int. J. Hydrog. Energy* **2019**, *44*, 29092–29099. [[CrossRef](#)]
21. Deveau, N.D.; Yen, P.-S.; Datta, R. Evaluation of hydrogen sorption and permeation parameters in liquid metal membranes via Sieverts' apparatus. *Int. J. Hydrog. Energy* **2018**, *43*, 19075–19090. [[CrossRef](#)]
22. Mueller, W.M.; Blackledge, J.P.; Libowitz, G.G. *Metal Hydrides*; Academic Press: New York, NY, USA, 1968; 804p.
23. Kudiiarov, V.N.; Kashkarov, E.B.; Syrtanov, M.S.; Lider, A.M. Hydrogen sorption by Ni-coated titanium alloy VT1-0. *Int. J. Hydrog. Energy* **2017**, *42*, 10604–10610. [[CrossRef](#)]
24. Poirier, D.R.; Geiger, G.H. Fick's Law and diffusivity of materials. In *Transport Phenomena in Materials Processing*; Springer: Cham, Switzerland, 2016; pp. 419–461. [[CrossRef](#)]
25. Oriani, R.A. The diffusion and trapping of hydrogen in steel. *Acta Metall.* **1970**, *18*, 147–157. [[CrossRef](#)]
26. Kudiiarov, V.N.; Pushilina, N.S.; Harchenko, S.Y. Development of stand for testing electrochemical permeation (STEP) of hydrogen through metal foils. *AMR* **2015**, *1085*, 224–228. [[CrossRef](#)]
27. Titov, A.I.; Lun-Fu, A.V.; Gayvaronskiy, A.V.; Bubenchikov, M.A.; Bubenchikov, A.M.; Lider, A.M.; Syrtanov, M.S.; Kudiiarov, V.N. Hydrogen accumulation and distribution in pipeline steel in intensified corrosion conditions. *Materials* **2019**, *12*, 1409. [[CrossRef](#)] [[PubMed](#)]
28. Shulepov, I.; Lomygin, A.; Roman, L.; Kashkarov, E.B.; Syrtanov, M.S. Correction of the distribution profiles of the intensities of elements considering the uneven dispersion of the glow-discharge optical emission spectrometer for multilayer coatings analysis. In Proceedings of the 7th International Congress on Energy Fluxes and Radiation Effects (EFRE), Tomsk, Russia, 4–26 September 2020; pp. 1155–1159. [[CrossRef](#)]
29. Li, L.; Song, B.; Cheng, J.; Yang, Z.; Cai, Z. Effects of vanadium precipitates on hydrogen trapping efficiency and hydrogen induced cracking resistance in X80 pipeline steel. *Int. J. Hydrog. Energy* **2018**, *43*, 17353–17363. [[CrossRef](#)]
30. Mohtadi-Bonab, M.A.; Szpunar, J.A.; Collins, L.; Stankievich, R. Evaluation of hydrogen induced cracking behavior of API X70 pipeline steel at different heat treatments. *Int. J. Hydrog. Energy* **2014**, *39*, 6076–6088. [[CrossRef](#)]
31. Huang, F.; Liu, J.; Deng, Z.J.; Cheng, J.H.; Lu, Z.H.; Li, X.G. Effect of microstructure and inclusions on hydrogen induced cracking susceptibility and hydrogen trapping efficiency of X120 pipeline steel. *Mater. Sci. Eng. A* **2010**, *527*, 6997–7001. [[CrossRef](#)]
32. Gan, L.; Huang, F.; Zhao, X.; Liu, J.; Cheng, Y.F. Hydrogen trapping and hydrogen induced cracking of welded X100 pipeline steel in H₂S environments. *Int. J. Hydrog. Energy* **2018**, *43*, 2293–2306. [[CrossRef](#)]